Quantitative x-ray magnetic circular dichroism microspectroscopy of Fe/Co/Cu(001) using a photoemission microscope

W. Kuch,[a] J. Gilles, S. S. Kang, F. Offi, and J. Kirschner
Max-Planck-Institut für Mikrostrukturphysik, Weinberg 2, D-06120 Halle, Germany

S. Imada and S. Suga
Osaka University, Graduate School of Engineering Science, 1-3 Machikaneyama, Toyonaka 560-8531, Japan

Photoelectron emission microscopy is combined with soft x-ray magnetic circular dichroism (XMCD) absorption spectroscopy to obtain local element-resolved quantitative magnetic properties with microscopic resolution. This is applied to study 0–14 ML Fe wedges with a slope of 0.055 ML/μm on 6 ML Co/Cu(001). Local XMCD spectra at the Fe $L_{2,3}$ edge confirm the presence of three magnetically different thickness regions of Fe with effective spin moments of $2.5\mu_B$ (0–4.5 ML), $0.7\mu_B$ (4.5–11 ML), and $1.8\mu_B$ (>11 ML). The value of $0.7\mu_B$ in the second phase is consistent with an fcc Fe phase containing nonferromagnetic layers underneath a ferromagnetic surface. © *2000 American Institute of Physics.* [S0021-8979(00)44908-X]

Photoelectron emission microscopy (PEEM) in connection with resonant excitation by circularly polarized light has proven its usefulness for the study of magnetic microstructures and multilayers.[1,2] The lateral intensity distribution of emitted low energy secondary electrons is thereby magnified by an electron optics. The effect of soft x-ray magnetic circular dichroism (XMCD) provides the magnetic contrast. The absorption of circularly polarized photons at elemental absorption edges differs for different alignment of light helicity and magnetization direction,[3] leading to a difference in secondary electron intensity. Sum rules[4] allow one to extract spin and orbital magnetic moments from integrals in the difference curve of two absorption spectra for opposite light helicity.[5,6]

The combination of the principles of microscopy (PEEM) and spectroscopy (XMCD) unites the advantages of both methods, namely the element-selective quantitative information of electronic and magnetic properties of XMCD, and the lateral resolution of PEEM. It is what we call ''microspectroscopy,'' and results in images displaying quantitative magnetic properties on an element-resolved basis. Practically, this implies to scan the photon energy and record microscopic images of the secondary electron intensity for both helicities at each energy step. From such a set of images local XMCD spectra at any position in the image can be analyzed.

In this article we demonstrate the application of this PEEM–XMCD microspectroscopy to study the magnetic phases of Fe on fcc Co/Cu(001). A common means of efficiently studying the thickness dependence of thin film properties is to image their spatial distribution on wedge-shaped samples. For that purpose we deposited Fe as 0–14 ML microwedges on 6 ML Co/Cu(001), and obtained the full spectroscopic XMCD information of that wedge from the analysis of PEEM images.

Ultrathin epitaxial Fe films, grown at room temperature on Cu(001), are one of the most interesting systems with respect to the interplay between structural and magnetic properties.[7–11] For film thicknesses below ≈4 atomic monolayers (ML) a fully ferromagnetic fcc-like structure is present.[8] In the thickness range between 4 and 11 ML, a second phase, a relaxed fcc structure, is found with a nonferromagnetic behavior of the inner film layers, but ferromagnetism at the surface.[9] For thicknesses above ≈11 ML, a third phase appears, a ferromagnetic (011) oriented bcc phase.[10] Fe films grown on Co/Cu(001) exhibit a very similar sequence of structural and magnetic phases.[12–14] The main difference from Fe/Cu(001) concerns the direction of the easy magnetic axis, which is in-plane in the case of Fe/Co/Cu(001). As for the presence of the ferromagnetic surface layer in the second phase, controversial experimental evidence has been reported. While from oxygen adsorption[13] and XMCD experiments[12] it has been concluded that the surface is not ferromagnetic, other XMCD measurements[14] as well as measurements of photoelectron diffraction in magnetic dichroism[15] and spin-resolved valence band photoemission,[16] provided evidence for the presence of ferromagnetic surface layers on top of nonferromagnetic underlayers.

Co and Fe films were evaporated at room temperature by thermal evaporation. Before depositing the Fe wedge, the Co film was remanently magnetized by a field of 500 Oe in the [110] direction. The wedge-shaped Fe films were prepared by placing an aperture of $2\times0.5\,\mathrm{mm}^2$ in front of the sample,

[a]Author to whom correspondence should be addressed; electronic mail: kuch@port.exp.bessy.de

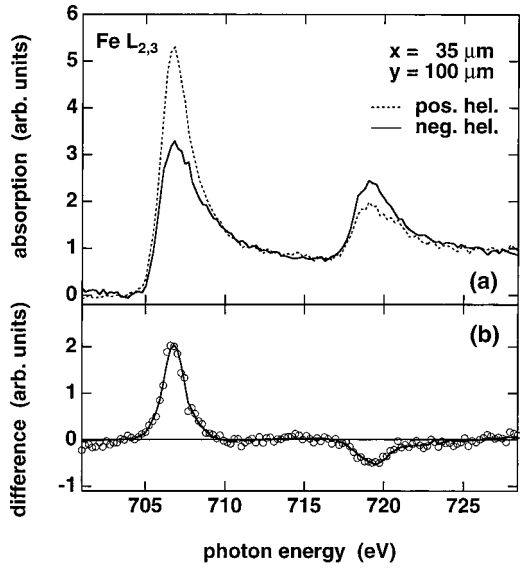

FIG. 1. (a) Fe $L_{2,3}$ absorption spectra of a single 1.5×3 μm^2 pixel at coordinates $x=35$ μm, $y=100$ μm. The dashed (solid) line depicts absorption for positive (negative) helicity. (b) Markers: Difference between the two curves of (a). Line: Template difference curve, obtained from averaging 1500 pixels in the region of bcc Fe, presented here with different scaling at the L_3 and L_2 edge to fit the single pixel data.

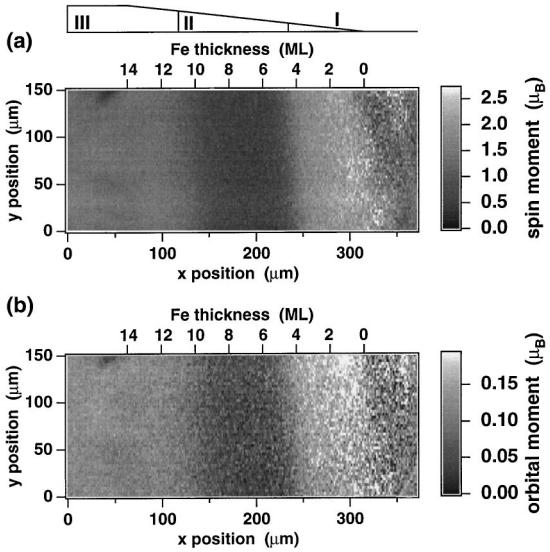

FIG. 2. Result of the pixel-by-pixel sum-rule analysis of the imaged area in Fe/6 ML Co/Cu(001): (a) Fe effective spin moment μ_S, (b) Fe orbital moment μ_L. Different levels of gray correspond to different values of μ_S and μ_L, as explained in the respective legend. Three different phases as schematically shown are characterized by different moments.

with a distance of 1 mm to the sample surface. During deposition the sample was rocked by $\pm7.5°$ about the long axis of the aperture. This results in a rectangle with two 255 μm broad wedges at the long sides, exhibiting slopes of 0.055 ML/μm.

The PEEM measurements were performed at beamline BL25SU of SPring-8 in Japan, which provides >95% circularly polarized light.[17] The light was incident under an angle of 30° to the sample surface, with an azimuthal angle of 18° to the [110] axis of the Cu substrate. The local photon energy resolution in the images is better than 150 meV. All images were normalized to the photoyield of the gold-coated refocusing mirror in front of the experimental chamber.

The setup of the photoemission microscope (Focus IS-PEEM)[18] is identical to that described in previous publications.[2] The contrast aperture was set to 70 μm for the present measurements. To obtain a large field of view, a low extraction voltage of about 200 V was used. This results in a lateral resolution of about 1 μm, and a field of view of about 380 μm. The magnified image is intensified by a two-stage multichannel plate, and converted into visible light by means of a scintillator crystal. The image is then computer-recorded with 12-bit resolution by a Peltier-cooled camera (PCO SensiCam).[19] Exposure time was 20 s/image, the total time for the acquisition of the over 3 million data points was about 1 h 50 min. The helicity was reversed once after completion of a full energy scan.

Figure 1(a) shows typical Fe $L_{2,3}$ absorption spectra of a single pixel of 1.5×3 μm^2 on the sample surface at 14 ML Fe thickness. The spectra are composed of information of that particular pixel from 242 different images. Dashed (solid) lines depict absorption for positive (negative) helicity. In panel (b) the corresponding difference is shown (open circles). The solid line gives the fit of a difference curve averaged from 1500 pixels at the thick end of the Fe wedge (bcc Fe). It serves as a template for the automated analysis of the 12 648 single pixel spectra. Only two parameters were used to fit that template difference curve to the single pixel difference curves. They describe the separate scaling of the L_3 and L_2 regions. Having analyzed the template XMCD spectra beforehand by means of the sum rules, sum-rule analysis of the single pixel data is obtained from these two fit parameters. This analysis is valid if the shape of the absorption spectra does not change over the imaged area. This was determined to be the case for the present Fe and Co images. The analysis of the template data was done as described elsewhere.[20] The data were corrected for the angle of incidence with respect to the [110] magnetization direction, and for the degree of light polarization. The number of Fe *d* holes was taken as 3.34.[21] For the analysis of the single pixel data the white line intensity was assumed to be proportional to the L_3 peak height. Only a smooth spatial variation of the white line intensity of less than 15% was present in the spectra over the imaged area. To avoid unreasonably long data acquisition times and contamination of the surface, the energy scans were taken only up to an energy of 728 eV. Part of the tail of the L_2 dichroism at higher photon energies is therefore not included in the analysis. This leads to systematic deviations of the magnetic moments as determined by the sum rules, predominantly of the orbital moment. A cutoff in the integration on the high energy side of the spectra leads to a higher apparent orbital moment.[22] From comparison with the curves for bulk Fe of Ref. 5 we estimate that the orbital moments will be affected by a factor of 2.6 ± 0.2, while the result for the effective spin moment is correct within 5%. To account for that, the orbital moments' values were corrected by a factor of 1/2.6.

Figure 2(a) shows the result of the pixel-by-pixel sum-rule analysis for the Fe effective spin moment μ_S. The Fe

thickness increases from right to left, as indicated. Different levels of gray correspond to different values of μ_S, as explained in the legend. The three different phases at Fe thicknesses of 0–4.5, 4.5–11, and >11 ML are clearly recognized by their different moments. The averaged values are $2.5\mu_B$ at 1.5–2 ML, $0.7\mu_B$ at 6–7 ML, and $1.8\mu_B$ above 14 ML. Analysis of Co $L_{2,3}$ microspectroscopy, seen through the Fe overlayer, revealed a constant value of $1.6\mu_B$ over the whole image.

In panel (b) the pixel-by-pixel analysis for the Fe orbital moment μ_L is shown. Compared to the spin moment [panel (a)] the noise is higher because μ_L is obtained from the difference between the areas of L_3 and L_2 dichroism, whereas they are summed for μ_S. The orbital moment qualitatively follows the spin moment through the sequence of the three different phases in the Fe wedge. The ratio of orbital to spin moment is roughly constant, with a slight change from 0.08 ± 0.01 in region I to 0.10 ± 0.01 in region III.

The Fe spin magnetic moments observed here agree qualitatively well with those found by Schmitz *et al.* ($3.0\mu_B$ in phase I, $1.1\mu_B$ in phase II),[14] although our values are systematically lower. The value of $0.7\mu_B$ in region II has to be interpreted as the depth-weighted average of all Fe layers. It is consistent with ferromagnetic Fe at the surface, for example, 2 ML ferromagnetic Fe ($2.2\mu_B$) on top of 6 ML nonferromagnetic Fe and a probing depth of 17 Å.[23] This contrasts with the result of Ref. 12, where a drop in the dichroism by a factor of about 10 between phase I and II was observed. $1.8\mu_B$ for bcc Fe is lower than the expected bulk value of $2.2\mu_B$. It is conceivable that the Fe films are even at 14 ML not yet entirely converted to the fully ferromagnetic bcc structure.

In conclusion, we have demonstrated how the combination of PEEM microscopy and XMCD spectroscopy can be used to obtain spectroscopic information on a microscopic scale. It allows the imaging of element-resolved local quantitative magnetic properties. Microspectroscopy of wedges or crossed double wedges can help significantly in the magnetic characterization of layered systems. Operating the photoemission microscope in high-resolution mode will open the way for the investigation of magnetic microstructures and microscopic domain structures by XMCD.

The authors are grateful for financial support by the BMBF (Grant No. 05 SL8EF1 9), JSPS, and DFG (Grant Nos. Ki 358/3-1 and 446 JAP-113/179/0). They would like to thank B. Zada for assistance in shipping the equipment and for dealing with custom's procedures. The experiments were performed at SPring-8 with the approval and financial support of JASRI (Proposal No. 1999A0319-NS-np). They extend special thanks to the SPring-8 staff, in particular Y. Saitoh and R.-J. Jung, for generous help during the beamtime.

[1] J. Stöhr, Y. Wu, M. G. Samant, B. B. Hermsmeier, G. Harp, S. Koranda, D. Dunham, and B. P. Tonner, Science **259**, 658 (1993).
[2] W. Kuch, R. Frömter, J. Gilles, D. Hartmann, Ch. Ziethen, C. M. Schneider, G. Schönhense, W. Swiech, and J. Kirschner, Surf. Rev. Lett. **5**, 1241 (1998); W. Swiech *et al.*, J. Electron Spectrosc. Relat. Phenom. **84**, 171 (1997); C. M. Schneider, J. Magn. Magn. Mater. **175**, 160 (1997).
[3] J. L. Erskine and E. A. Stern, Phys. Rev. B **12**, 5016 (1975); G. Schütz, W. Wagner, W. Wilhelm, P. Kienle, R. Zeller, R. Frahm, and G. Materlik, Phys. Rev. Lett. **58**, 737 (1987).
[4] B. T. Thole, P. Carra, F. Sette, and G. van der Laan, Phys. Rev. Lett. **68**, 1943 (1992); P. Carra, B. T. Thole, M. Altarelli, and X. Wang, *ibid.* **70**, 694 (1993).
[5] C. T. Chen, Y. U. Idzerda, H.-J. Lin, N. V. Smith, G. Meigs, E. Chaban, G. H. Ho, E. Pellegrin, and F. Sette, Phys. Rev. Lett. **75**, 152 (1995).
[6] J. Stöhr, J. Electron Spectrosc. Relat. Phenom. **75**, 253 (1995).
[7] J. Thomassen, F. May, B. Feldmann, M. Wuttig, and H. Ibach, Phys. Rev. Lett. **69**, 3831 (1992).
[8] M. T. Kief and W. F. Egelhoff, Jr., Phys. Rev. B **47**, 10785 (1993); K. Heinz, S. Müller, and P. Bayer, Surf. Sci. **337**, 215 (1995).
[9] P. Bayer, S. Müller, P. Schmailzl, and K. Heinz, Phys. Rev. B **48**, 17611 (1993); D. Li, M. Freitag, J. Pearson, Z. Q. Qiu, and S. D. Bader, Phys. Rev. Lett. **72**, 3112 (1994); S. Müller, P. Bayer, A. Kinne, P. Schmailzl, and K. Heinz, Surf. Sci. **322**, 21 (1995); M. Straub, R. Vollmer, and J. Kirschner, Phys. Rev. Lett. **77**, 743 (1996).
[10] M. Wuttig, B. Feldmann, J. Thomassen, F. May, H. Zillgen, A. Brodde, H. Hannemann, and H. Neddermayer, Surf. Sci. **291**, 14 (1993); J. Giergiel, J. Kirschner, J. Landgraf, J. Shen, and J. Woltersdorf, *ibid.* **310**, 1 (1994); J. Giergiel, J. Shen, J. Woltersdorf, A. Kirilyuk, and J. Kirschner, Phys. Rev. B **52**, 8528 (1995).
[11] M. Zharnikov, A. Dittschar, W. Kuch, C. M. Schneider, and J. Kirschner, Phys. Rev. Lett. **76**, 4620 (1996); J. Magn. Magn. Mater. **174**, 40 (1997).
[12] W. L. O'Brien and B. P. Tonner, Surf. Sci. **334**, 10 (1995); Phys. Rev. B **52**, 15332 (1995).
[13] E. J. Escorcia-Aparicio, R. K. Kawakami, and Z. Q. Qiu, Phys. Rev. B **54**, 4155 (1996).
[14] D. Schmitz, C. Charton, A. Scholl, C. Carbone, and W. Eberhardt, Phys. Rev. B **59**, 4327 (1999).
[15] X. Gao, M. Salvietti, W. Kuch, C. M. Schneider, and J. Kirschner, Phys. Rev. B **58**, 15426 (1998).
[16] R. Kläsges, D. Schmitz, C. Carbone, W. Eberhardt, and T. Kachel, Solid State Commun. **107**, 13 (1998).
[17] Y. Saitoh *et al.*, J. Synchrotron Radiat. **5**, 542 (1998).
[18] FOCUS GmbH, Am Birkhecker Berg 20, D-65510 Hünstetten, Germany.
[19] PCO Computer Optics GmbH, Ludwigsplatz 4, D-93309 Kelheim, Germany.
[20] W. Kuch, M. Salvietti, X. Gao, M.-T. Lin, M. Klaua, J. Barthel, C. V. Mohan, and J. Kirschner, Phys. Rev. B **58**, 8556 (1998); W. Kuch, M. Salvietti, X. Gao, M. Klaua, J. Barthel, C. V. Mohan, and J. Kirschner, J. Appl. Phys. **83**, 7019 (1998).
[21] R. Wu and A. J. Freeman, Phys. Rev. Lett. **73**, 1994 (1994).
[22] S. Imada, T. Muro, T. Shishidou, S. Suga, H. Maruyama, K. Kobayashi, H. Yamazaki, and T. Kanomata, Phys. Rev. B **59**, 8752 (1999).
[23] R. Nakajima, J. Stöhr, and Y. U. Idzerda, Phys. Rev. B **59**, 6421 (1999).